RadioGraphics

Rotator Cuff Tears: Clinical, Radiographic, and US Findings[1]

Josh B. Moosikasuwan, MD • Theodore T. Miller, MD • Brian J. Burke, MD

ONLINE-ONLY CME

See www.rsna.org/education/rg_cme.html.

LEARNING OBJECTIVES

After reading this article and taking the test, the reader will be able to:

- Discuss the most useful clinical and radiologic tests for rotator cuff tears.
- Describe US assessment for rotator cuff tears.
- Develop a differential diagnosis for shoulder pain and identify clinical mimics of rotator cuff tears.

Rotator cuff tears are a common cause of shoulder pain. Clinical and radiographic findings can suggest the presence of a rotator cuff tear. The most sensitive clinical findings are impingement and the "arc of pain" sign. Radiographic findings are usually normal in the acute setting, although the "active abduction" view may show decreased acromiohumeral distance. In more chronic cases, an outlet view may show decreased opacity and decreased size of the supraspinatus muscle due to atrophy. In late cases, the humeral head may become subluxated superiorly, and secondary degenerative arthritis of the glenohumeral joint may ensue. Ultrasonography (US), with over 90% sensitivity and specificity, can help confirm the diagnosis in clinically or radiographically equivocal cases. US can also reveal the presence of other abnormalities that may mimic rotator cuff tear at clinical examination, including tendinosis, calcific tendinitis, subacromial subdeltoid bursitis, greater tuberosity fracture, and adhesive capsulitis.

RadioGraphics 2005; 25:1591–1607 • **Published online** 10.1148/rg.256045203 • **Content Codes:** MK US

[1]From the Department of Radiology, North Shore University Hospital, 825 Northern Blvd, Great Neck, NY 11021. Presented as an education exhibit at the 2003 RSNA Annual Meeting. Received November 16, 2004; revision requested January 4, 2005, and received January 28; accepted January 31. All authors have no financial relationships to disclose. **Address correspondence to** T.T.M. (e-mail: *tmiller@nshs.edu*).

Introduction

Crass et al (1) and Middleton et al (2) in 1984 were the first to describe ultrasonographic (US) evaluation for rotator cuff tears, and US has proved to be as accurate as magnetic resonance (MR) imaging in the detection of supraspinatus tendon tears. In a recent study comparing US with MR imaging and using arthroscopy as the standard of reference, Teefey et al (3) demonstrated an overall accuracy of 87% for both modalities in correctly identifying partial- and full-thickness rotator cuff tears as well as the absence of such tears. In that study, US helped correctly identify 45 of 46 full-thickness tears and 13 of 19 partial-thickness tears, whereas MR imaging helped correctly identify all 46 full-thickness tears and 12 of 19 partial-thickness tears. The reported accuracy, sensitivity, and specificity of US in the detection of any tear, whether partial or full thickness, are all greater than 90% (3–5).

However, even before advanced imaging (eg, MR imaging, US) is performed, the diagnosis of rotator cuff tear can be suggested at clinical examination (6–9) and with radiography of the shoulder. In this article, we review the clinical, radiographic, and US evaluation of rotator cuff tears with an emphasis on US technique and the interpretation of US findings. We also discuss and illustrate a variety of conditions that can mimic rotator cuff tears clinically, including supraspinatus tendinosis, calcific tendinitis, subacromial subdeltoid bursitis, greater tuberosity fracture, and adhesive capsulitis.

Clinical Evaluation

Patient age is important because the prevalence of tears increases with age. Approximately 40% of asymptomatic patients over 50 years old have full-thickness rotator cuff tears (10), and the prevalence of partial- and full-thickness tears in symptomatic patients over 60 years old is greater than 60% (9). Chronic causes such as repetitive microtrauma, subacromial impingement, tendon degeneration, and hypovascularity are thought to be responsible for most tears and account for this age-dependent prevalence. Acute macrotrauma is less frequently responsible for tears (11,12).

Dinnes et al (8) recently reviewed 10 cohort studies on the clinical evaluation of the shoulder. Pooled data from four of these studies suggested that clinical examination as a whole has a sensitivity of 90% and a specificity of 54% in the detection of full-thickness rotator cuff tears. Although 23 different signs, symptoms, and tests were assessed in the 10 studies, no definite conclusion about individual tests could be reached, since too few studies evaluated any one test. In addition, there is some variability in how individual tests are performed (8). Nevertheless, a few studies have identified the most useful clinical tests for rotator cuff tears. Murrell and Walton (9) reviewed 23 clinical examinations for rotator cuff tears and found that supraspinatus weakness, weakness of external rotation, and impingement were the most useful indicators. If all three signs are positive, or if two signs are positive and the patient is at least 60 years old, the chance of partial- or full-thickness rotator cuff tear is 98%. Similarly, Litaker et al (7) showed that weakness of external rotation, patient age of at least 65 years, and night pain best helped predict the presence of partial- or full-thickness rotator cuff tear. Other clinical findings that these authors found most useful included weakness of abduction, impingement, and the "arc of pain" sign (pain during descent of the abducted arm). Weakness of external rotation, night pain, weakness of abduction, impingement, and the arc of pain sign had a sensitivity and a positive predictive value of 76% and 79%, 88% and 70%, 64% and 78%, 97% and 67%, and 98% and 67%, respectively (7). Weakness of abduction, impingement, and the arc of pain sign should be expected because rotator cuff tears usually involve the supraspinatus tendon. Weakness of external rotation is a sign of infraspinatus tear.

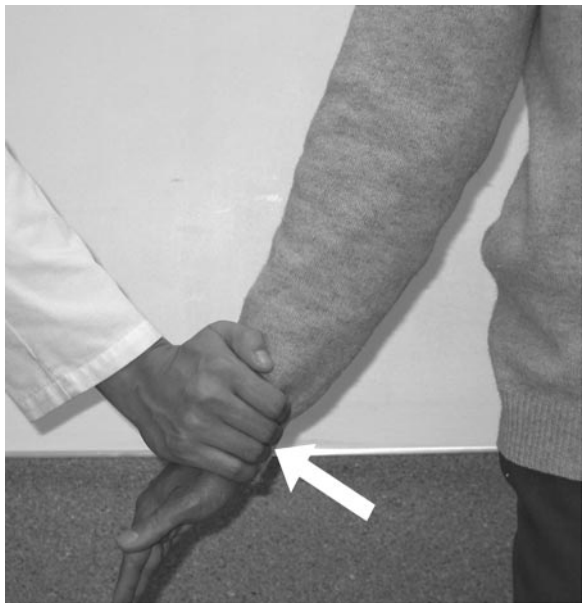

Figure 1. Clinical photograph illustrates evaluation for supraspinatus muscle weakness. With the elbow straight and the arm in 20° abduction, the patient is asked to abduct the arm (arrow) against an applied resistance.

The supraspinatus muscle aids not only in stabilization of the shoulder joint but also in abduction of the arm. To test for weakness, the patient's arm is straightened and then abducted 20°.

a. b.

Figure 2. Clinical photographs illustrate evaluation for impingement. **(a)** The examiner fully elevates the patient's arm (to at least 170°). **(b)** Next, the patient's humerus is internally rotated (arrow) and adducted against the ear. Afterward, the humerus is externally rotated and adducted against the ear (not shown). If there is increased pain with rotation in either direction, the test is positive.

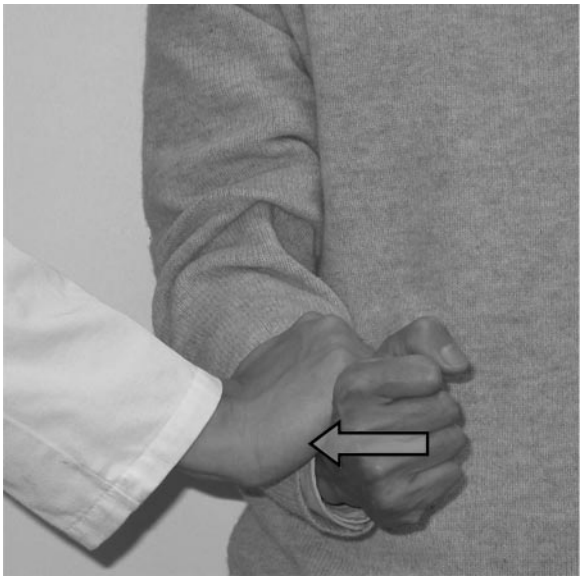

Figure 3. Clinical photograph illustrates evaluation for external rotation weakness. The patient's elbow is flexed 90°, and the shoulder is internally rotated 20°. The examiner then places his or her hand outside the patient's wrist and asks the patient to resist (arrow) an inward force.

The patient is then asked to abduct the arm against an applied force (Fig 1). Alternatively, supraspinatus strength can be assessed with the arm in the "empty can" (Jobe test) or "full can" position, the arm being elevated 90° in the scapular plane. In the empty can position, the arm is in full internal rotation with the thumb pointed down, whereas in the full can position, the arm is in 45° external rotation with the palm facing up (13).

Clinical impingement syndrome is characterized by pain during use of the shoulder that is relieved by local subacromial anesthetic injection. The pain can be due to *(a)* subacromial impingement from, for example, osteophytes (outlet impingement) (14) or *(b)* intraarticular causes such as underlying instability or labral lesions (nonoutlet impingement) (15). To test for impingement, the patient's arm is passively elevated to at least 170°, which maximizes contact between the acromion and underlying structures. The arm is then internally and externally rotated while adducted against the ear. If there is increased pain with either internal or external rotation, the test is positive (Fig 2). In addition, assessment for the arc of pain sign may be performed by having the patient actively lower the arm in the abduction plane. The test is positive when the pain is minimal at full elevation and increases as the arm descends, being maximal between 70° and 120° of abduction.

Another way to test for overhead impingement involves stabilizing the scapula and then elevating the patient's arm in a plane midway between the coronal and sagittal planes (Neer test) (16,17). The Hawkins test can also be performed. In this test, the arm is flexed to 90° and then internally rotated with the elbow bent slightly (16,18). Both tests are positive if there is pain, and both have high sensitivity (80%–90%) but low specificity for rotator cuff tears.

In contrast to most other tests of the shoulder, the drop-arm test has high specificity (98%) but low sensitivity (10%) for rotator cuff rupture (9,19). In this test, the patient is asked to actively abduct the arm to 90° and then to slowly lower the arm. If the arm drops abruptly with accompanying pain, the test is positive, with a 98% chance of a rotator cuff tear (9,19).

To test for weakness of external rotation (ie, by evaluating the infraspinatus and teres minor muscles), the patient is positioned with the elbow flexed 90° and the shoulder internally rotated 20°. The patient is then asked to resist an inward force (Fig 3).

Finally, the lift-off test can be performed to evaluate the subscapularis (20). This test is performed by passively positioning the patient's arm behind the back with the palm facing outward (Fig 4). Failure to hold the forearm and hand off the back or inability to push off against the examiner's hand constitutes a positive test. In their report on 16 patients with isolated subscapularis tendon tears, Gerber and Krushell (20) noted that 13 patients were unable to hold the forearm off the back, whereas three were unable to push off against the examiner's hand. Weakness of internal rotation is not a reliable indicator of subscapularis tear because there are other internal rotators of the humerus, such as the pectoralis muscle.

Figure 4. Clinical photograph illustrates evaluation for subscapularis tear. The patient's arm is passively positioned behind the back with the palm facing outward. The patient is then asked to lift the hand away from the back or push off against resistance.

Radiographic Evaluation

Impingement can be suggested radiographically by abnormalities that encroach upon the supraspinatus outlet. For example, spur formation on the undersurface of the acromioclavicular joint and an acromion with an inferolateral tilt can be seen on anteroposterior radiographs of the shoulder (21,22). In addition, a type III acromion, in which the anterior aspect of the acromion is hooked inferiorly, can be seen on a supraspinatus outlet view (a modified Y view) and has been associated with a higher prevalence of rotator cuff tears (Fig 5) (23,24).

Standard shoulder radiographs are usually normal in acute rotator cuff tears (25). However, an active abduction view, for which the patient abducts the shoulder to 90° or to the maximum extent possible, can be obtained to look for decreased acromiohumeral distance (≤2 mm) (25). The unopposed action of the deltoid muscle actively pulling the humerus superiorly and the absence of the supraspinatus as a physical barrier due to tear and retraction of the tendon are the basis for the decreased acromiohumeral distance.

The density and contour of the supraspinatus muscle on a supraspinatus outlet view can also be used to predict the presence of a tear (26). The supraspinatus muscle should normally have homogeneous soft-tissue density and a bulging superior contour (Fig 5). A flattened or ill-defined superior contour and a heterogeneous appearance of the muscle due to low-density fatty areas are 85% and 80% accurate for tear, respectively (26).

Without the supraspinatus to stabilize the humerus and oppose the upward traction exerted on the humerus by the deltoid muscle, the humerus eventually migrates superiorly, and a high-riding humeral head (acromiohumeral distance <7 mm) can be seen on an anteroposterior radiograph of the shoulder (27). In chronic rotator cuff tears, repetitive contact between the humeral head and the acromion can occur, resulting in remodeling and irregularity of these structures, particularly of the greater tuberosity. This condition is sometimes referred to as cuff arthropathy and can manifest as sclerosis, subchondral cysts, osteolysis, and notching or pitting of the greater tuberosity, usually with matching sclerosis and faceting or concavity in the inferolateral aspect of the acromion (28,29). With time, secondary osteophytosis in the glenohumeral joint can develop as a compensatory mechanism to maintain joint congruity (Fig 6) (28,30).

US Evaluation

US Technique

The technique for shoulder US and the typical US findings in rotator cuff tears have been described previously (11,12,31–33). A high-frequency (preferably 10–12-MHz) linear transducer is used. Tissue harmonic imaging can also be used because it has been shown to increase the conspicuity of tears, although not diagnostic accuracy (34). The ultrasound beam should be per-

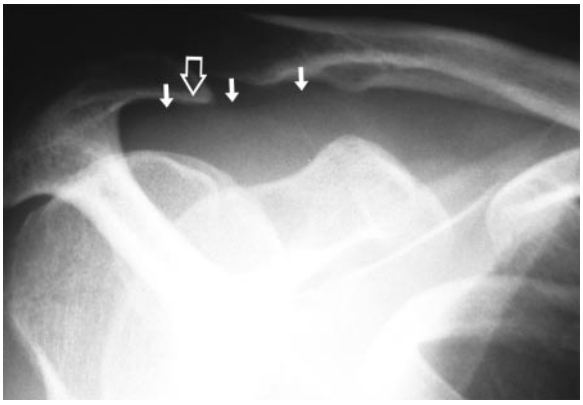

Figure 5. Radiograph (supraspinatus outlet view) shows the normal supraspinatus muscle, which has a homogeneous appearance with a bulging superior contour (solid arrows). Note also the type III acromion (open arrow).

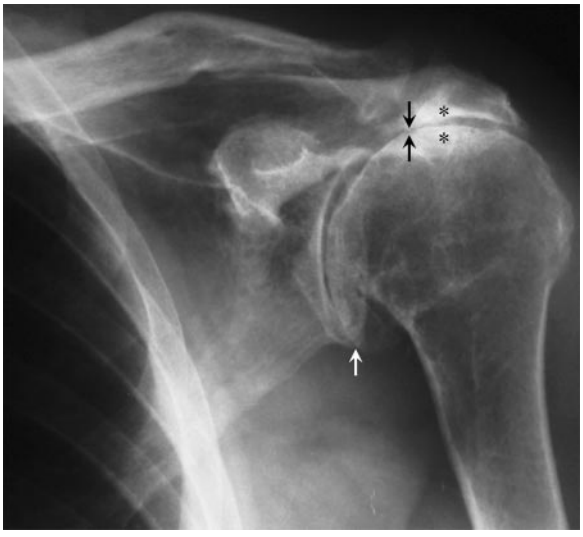

Figure 6. Chronic rotator cuff tear. Anteroposterior radiograph demonstrates a high-riding humerus with decreased acromiohumeral distance (black arrows). Secondary cuff arthropathy is also seen, manifesting as faceting and sclerosis in the inferolateral aspect of the acromion and the superior aspect of the greater tuberosity (*). Note also the osteophytosis arising from the humerus (white arrow).

pendicular to the tendon because even slight angulation can create artifactual hypoechoic to anechoic defects simulating tears (see Fig 8c). This artifact is called anisotropy, a phenomenon that is created when the interrogating ultrasound beam is not perpendicular to the highly organized parallel tendon fibers.

The US examination begins with evaluation of the biceps and subscapularis, then of the supraspinatus, and finally of the posterior structures, including the infraspinatus, teres minor muscle, and posterior glenohumeral joint. At our institution, the patient is seated on a stretcher facing the examiner, although some examiners prefer to scan from the side or from behind the patient. The clavicle, acromioclavicular joint, and spine of the scapula are useful bone landmarks.

Figure 7. Clinical photograph illustrates patient positioning for US evaluation of the long head of the biceps tendon. The forearm is supinated and placed on the thigh, bringing the bicipital groove (black line) forward.

Figure 7 demonstrates positioning for US evaluation of the biceps tendon. The forearm is supinated and placed on the thigh, bringing the bicipital groove forward. In the transverse plane, the biceps tendon is seen in the bicipital groove between the greater and lesser tuberosities (Fig 8). Turning the transducer longitudinally makes the biceps tendon appear as hyperechoic fibrillar lines interposed between the deltoid muscle and the humerus (Fig 9). The tendon can be followed from its musculotendinous junction to and then around the humeral head.

Figures 8, 9. **(8)** Transverse view of the long head of the biceps tendon. **(a)** Clinical photograph illustrates the US transducer oriented transverse to the longitudinal course of the tendon (dashed line). Solid line indicates the clavicle. **(b)** US image shows the biceps tendon (arrows) in the bicipital groove between the greater *(G)* and lesser *(L)* tuberosities. **(c)** US image obtained with the ultrasound beam not perpendicular to the tendon (arrows) demonstrates anisotropy, in which the tendon appears artifactually hypoechoic to anechoic. **(9)** Longitudinal view of the long head of the biceps tendon. **(a)** Clinical photograph illustrates the US transducer oriented longitudinal to the tendon. Black line indicates the clavicle. **(b)** On a US image, the biceps tendon (arrows) manifests as echogenic fibrillar lines interposed between the deltoid muscle *(D)* and the humerus *(H)*.

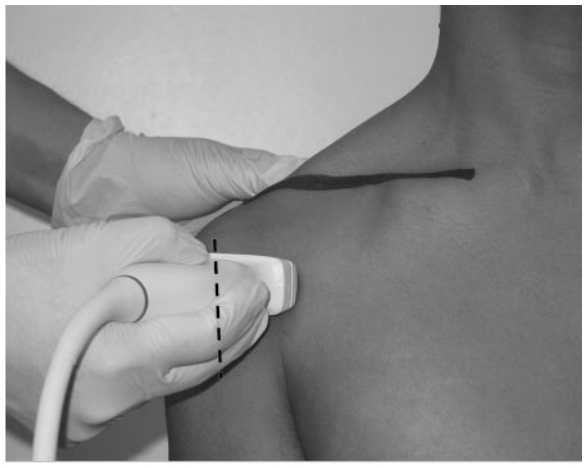

8a.

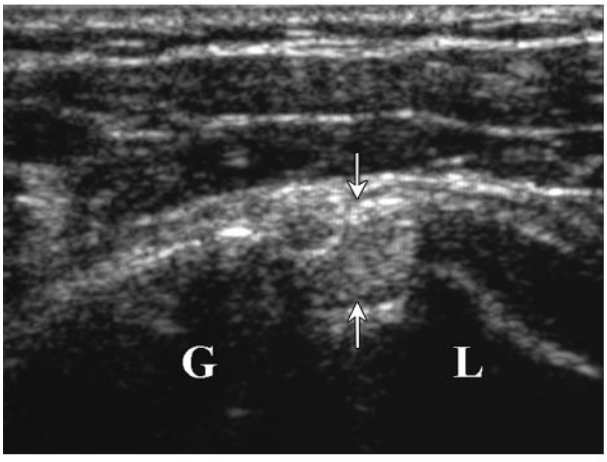

8b.

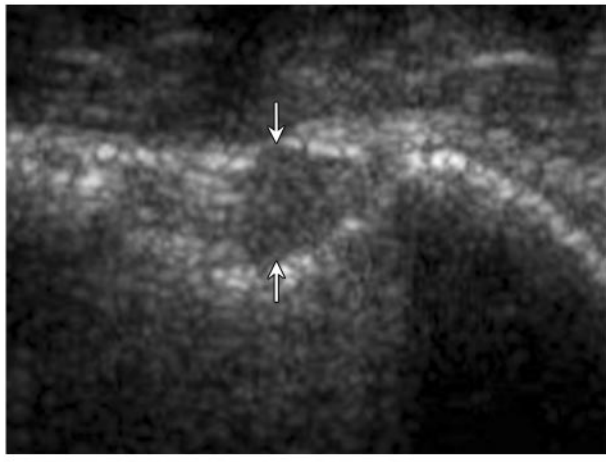

8c.

9a.

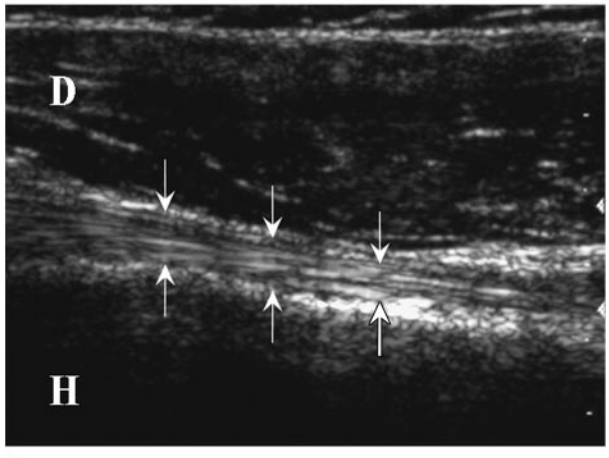

9b.

To evaluate the subscapularis tendon, the patient's arm is externally rotated, making sure to keep the elbow as close to the body as possible (Fig 10). This maneuver brings the tendon into a more anterior position. Rotating the transducer 90° so that it is oriented transverse to the arm allows the longitudinal extent of the subscapularis tendon to be seen as the tendon inserts on the lesser tuberosity (Fig 11). Some fibers extend across the bicipital groove to form the transverse humeral ligament, which anchors the extraarticular portion of the long head of the biceps tendon in place. On transverse images, the individual tendon slips of the subscapularis tendon can be seen (Fig 12).

Figure 10. Clinical photograph illustrates patient positioning for US evaluation of the subscapularis tendon. The arm is externally rotated, bringing the tendon (black box) into a more anterior position.

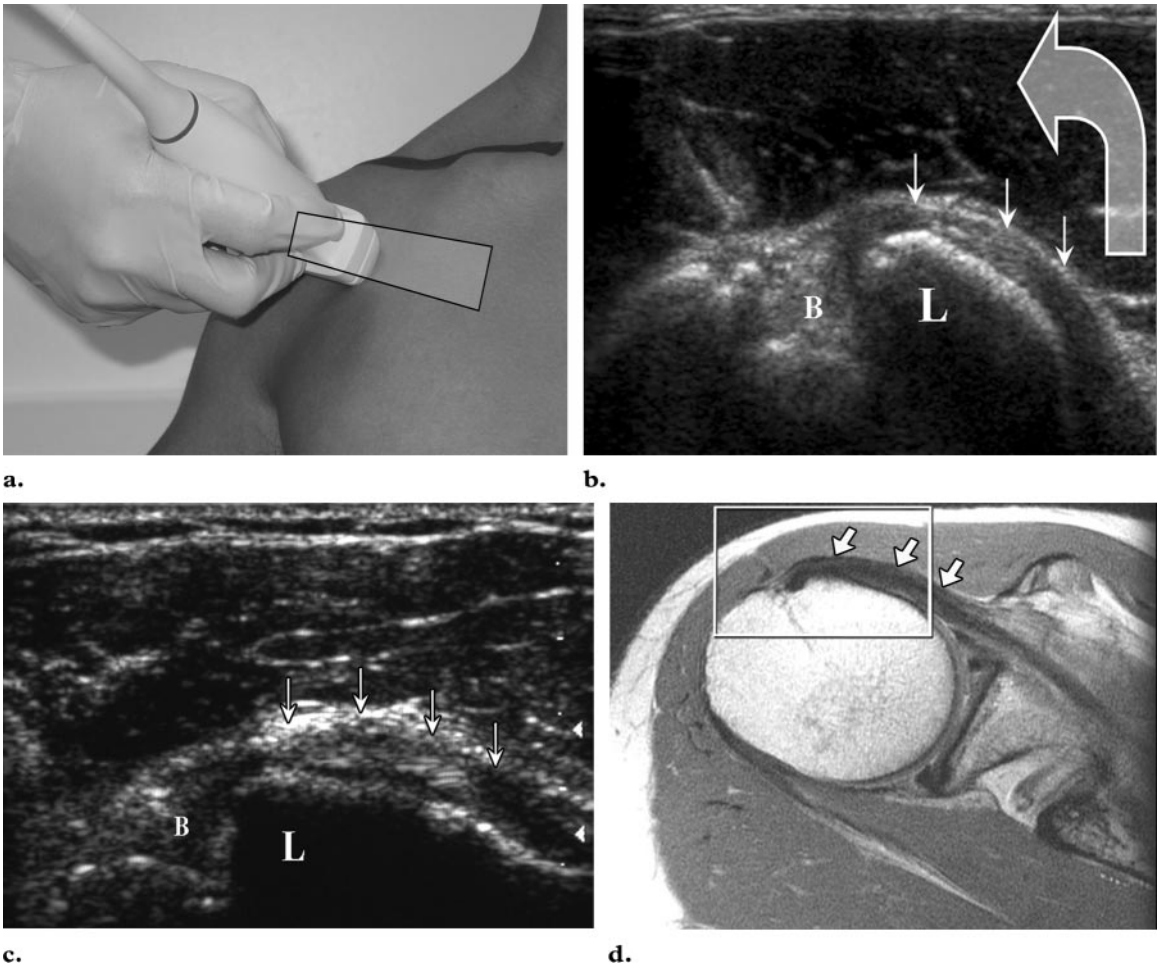

Figure 11. Longitudinal view of the subscapularis tendon. **(a)** Clinical photograph illustrates the US transducer oriented transverse to the arm but longitudinal to the subscapularis tendon (shaded box). **(b, c)** On US images, the subscapularis tendon (small arrows in **b**, arrows in **c**) is seen at its insertion site on the lesser tuberosity *(L)* and extending to the bicipital groove *(B)*. By externally rotating the humerus in the direction indicated by the large arrow in **b**, more of the tendon is brought into view (cf **c**). **(d)** Corresponding axial proton-density–weighted MR image also shows the subscapularis tendon (arrows). The box corresponds to the field of view in the US images.

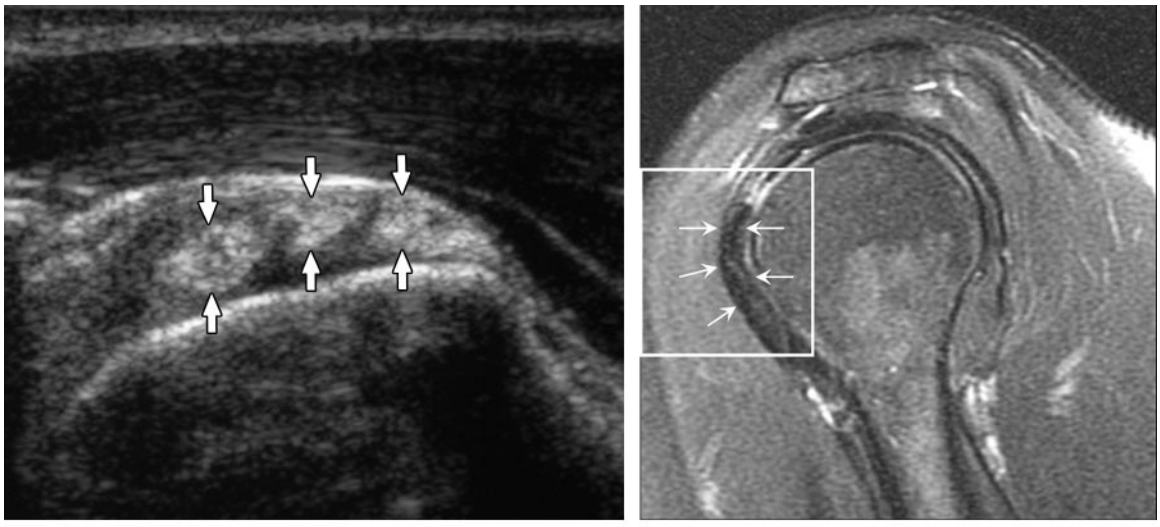

a. b.

Figure 12. Transverse view of the subscapularis tendon. US image **(a)** and corresponding sagittal oblique fat-suppressed T2-weighted MR image **(b)** show the subscapularis tendon (arrows in **b**). Note the echogenic tendon slips (arrows in **a**). The box in **b** corresponds to the field of view in **a**.

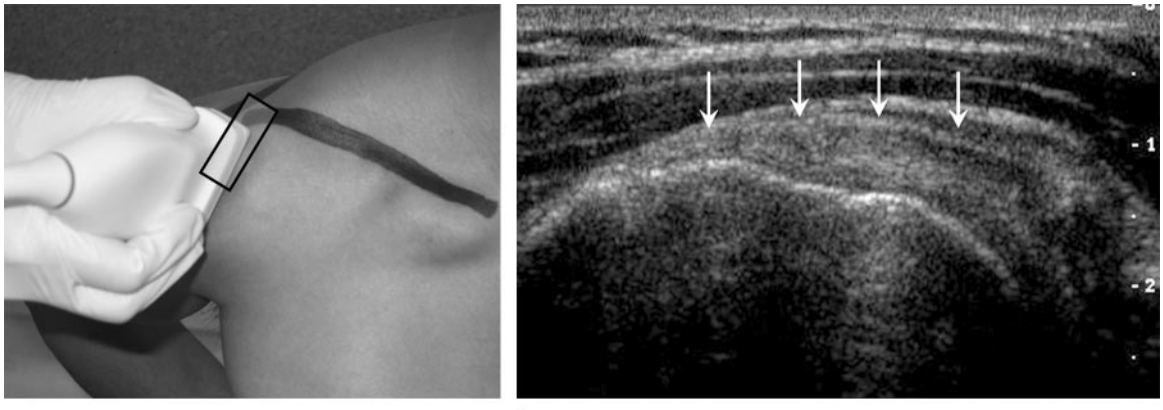

a. b.

Figure 14. Longitudinal view of the supraspinatus tendon. **(a)** Clinical photograph illustrates the US transducer placed anterior to the acromioclavicular joint and roughly parallel to the spine of the scapula (black line on top of shoulder) for longitudinal evaluation of the supraspinatus tendon (shaded box). Black line on front of shoulder indicates the clavicle. **(b, c)** US image **(b)** and corresponding coronal oblique proton-density–weighted MR image **(c)** demonstrate the supraspinatus tendon (arrows). The box in **c** corresponds to the field of view in **b**.

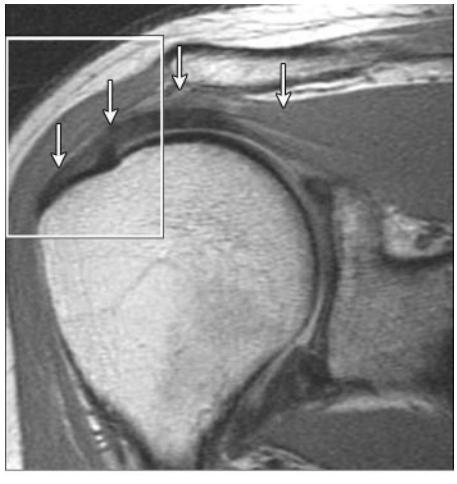

c.

For visualization of the supraspinatus tendon, the patient's hand is placed either behind the back or on the buttock with the elbow pointed posteriorly (Fig 13). This position exposes the supraspinatus tendon by bringing it out from underneath the acromioclavicular joint and brings into view the insertion of the tendon on the superior aspect of the greater tuberosity. The US transducer should be oriented 45°, or approximately midway between the coronal and sagittal planes, to demonstrate the longitudinal course of the supraspinatus tendon. The course of the spine of the scapula is a useful reference plane (Fig 14). The transducer is then rotated 90° to demonstrate the tendon in the transverse plane (Fig 15).

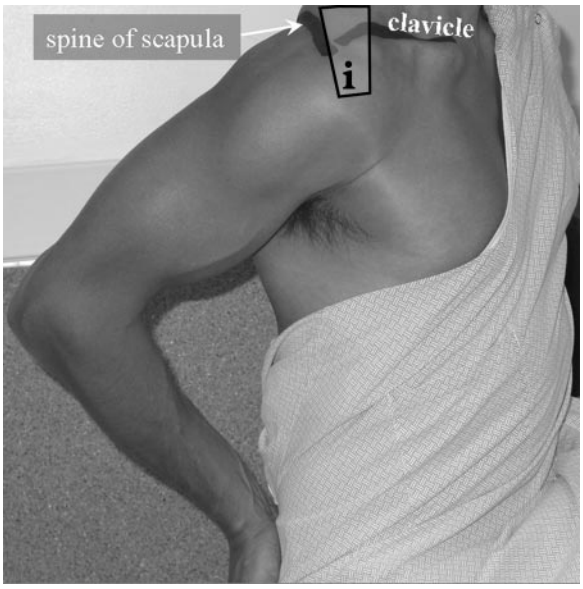

Figure 13. Clinical photograph illustrates patient positioning for US evaluation of the supraspinatus tendon. The hand is placed on the buttock with the elbow pointed backward, bringing the insertion site *(i)* of the supraspinatus tendon (shaded box) on the superior aspect of the greater tuberosity out from beneath the acromion and into view.

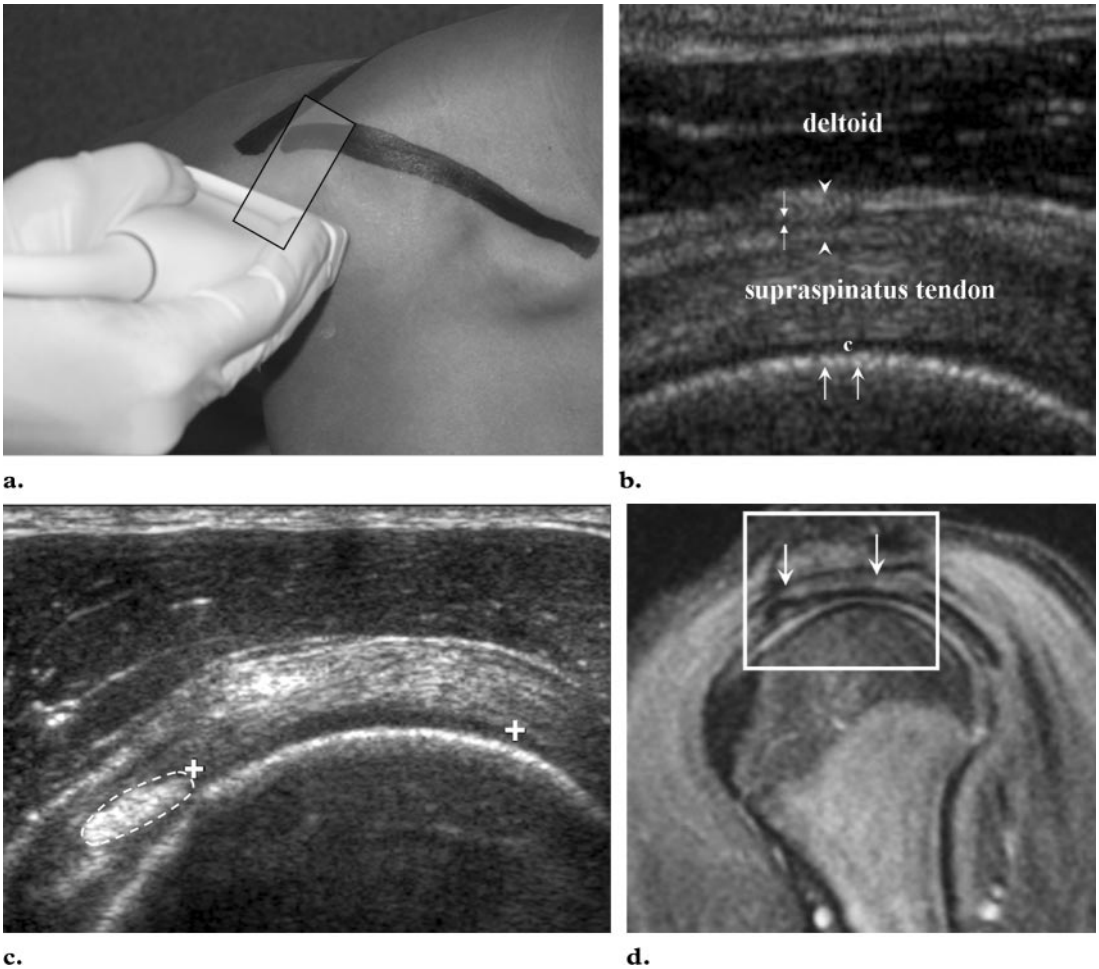

Figure 15. Transverse view of the supraspinatus tendon. **(a)** Photograph shows transducer position for transverse evaluation of the supraspinatus tendon (box). The transducer is turned 90° (cf Fig 14a). Black lines indicate the spine of the scapula and the clavicle. **(b)** Transverse US image of the shoulder shows the deltoid muscle, peribursal fat (arrowheads) surrounding the subacromial subdeltoid bursa (small arrows), the supraspinatus tendon, and the cartilage *(c)* and underlying cortex of the humerus (large arrows). **(c)** US image shows how moving the transducer more anteriorly and inferiorly around the humeral head curvature brings the round hyperechoic biceps tendon (dashed oval) into view. About 2.0–2.5 cm of tendon posterior to the biceps tendon is the supraspinatus tendon (cursors), with the infraspinatus tendon more posterior. **(d)** Sagittal oblique fat-suppressed proton-density–weighted MR image shows the supraspinatus tendon in the transverse plane (arrows). Box corresponds to field of view in **b**.

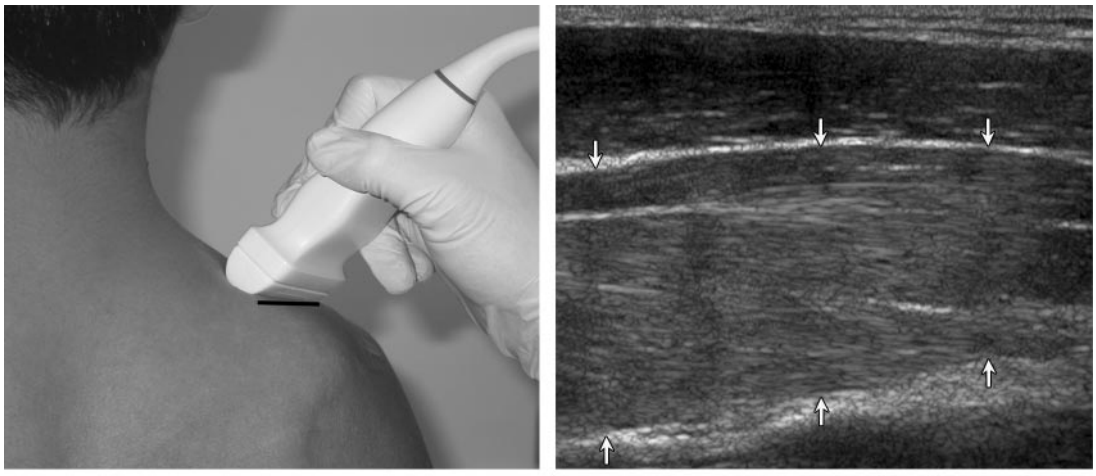

a. b.

Figure 16. Longitudinal view of the supraspinatus muscle. **(a)** Clinical photograph illustrates the transducer placed in the supraspinatus fossa, anterior and parallel to the spine of the scapula (black line). **(b)** US image shows the supraspinatus muscle (arrows) interposed between the trapezius muscle and the scapula.

In this plane, the deltoid muscle, which is hypoechoic in hyperechoic fascial planes, is just deep to the subcutaneous fat. Underneath the deltoid muscle is the anechoic subacromial subdeltoid bursa surrounded by hyperechoic peribursal fat. The supraspinatus tendon appears hyperechoic and fibrillar and sits directly on the humerus. A thin anechoic rim of cartilage covers the hyperechoic bone cortex.

Moving the transducer anteriorly around the curvature of the humeral head in the oblique transverse plane allows visualization of the hyperechoic biceps tendon. The biceps tendon is used as a reference point for determining the location and size of tears. The supraspinatus tendon is the 2.0–2.5 cm of cuff tissue immediately posterior to the biceps tendon, with the infraspinatus tendon more than 2.5 cm posterior (Fig 15c). To evaluate the supraspinatus muscle, the transducer is positioned anterior and parallel to the spine of the scapula in the supraspinatus fossa (Fig 16).

Finally, the infraspinatus muscle and tendon and the posterior glenohumeral joint are evaluated. The arm is placed in the same position as that used for evaluation of the biceps tendon. The transducer is positioned just inferior and parallel to the spine of the scapula, bringing the infraspinatus muscle into view. The infraspinatus muscle is then followed laterally as it crosses the posterior glenohumeral joint and becomes the tendon. The evaluation of the infraspinatus tendon can be optimized with internal rotation of the humerus by having the patient reach for the opposite arm. The posterior labrum is also demonstrated by moving the transducer medially in this orientation and appears homogeneous, hyperechoic, and triangular (Fig 17).

On these posterior images, fluid in the axillary pouch and posterior recess of the glenohumeral joint can also be detected. The posterior recess is

a.

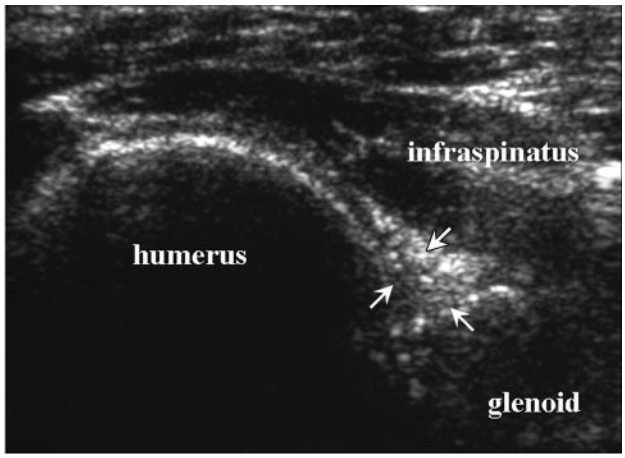

b.

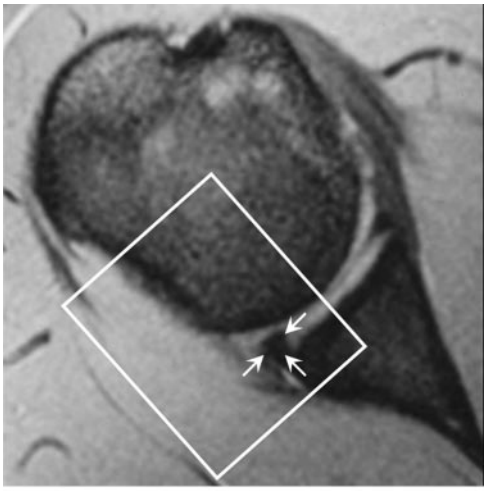

c.

Figure 17. Evaluation of the posterior aspect of the shoulder. **(a)** Clinical photograph illustrates the US transducer position. **(b, c)** US image **(b)** and axial gradient-echo MR image **(c)** show the posterior aspect of the glenohumeral joint. The normal posterior labrum (arrows) is homogeneously hyperechoic at US and hypointense at MR imaging. The box in **c** corresponds to the field of view in **b**.

deep to the infraspinatus tendon, whereas the axillary pouch lies along the inferior edge of the teres minor muscle. The appearance of fluid in the posterior recess can be accentuated by having the patient rotate the arm externally. The glenohumeral joint also communicates with the sheath of the long head of the biceps tendon, and fluid in the tendon sheath may indicate a joint effusion.

US Appearances of Disease

Tears of the rotator cuff tendons are classified as either full thickness or partial thickness. Full-thickness tears extend from the bursal surface to the articular surface. Partial-thickness tears are focal defects in the tendon that involve only the bursal or articular surface.

Full-thickness rotator cuff tears usually appear as hypoechoic or anechoic defects in which fluid has replaced the area of the torn tendon (Fig 18). Fluid in the region of the torn tendon can also allow increased through-transmission of the ultrasound beam, accentuating the appearance of the underlying cartilage. Thus, two hyperechoic lines

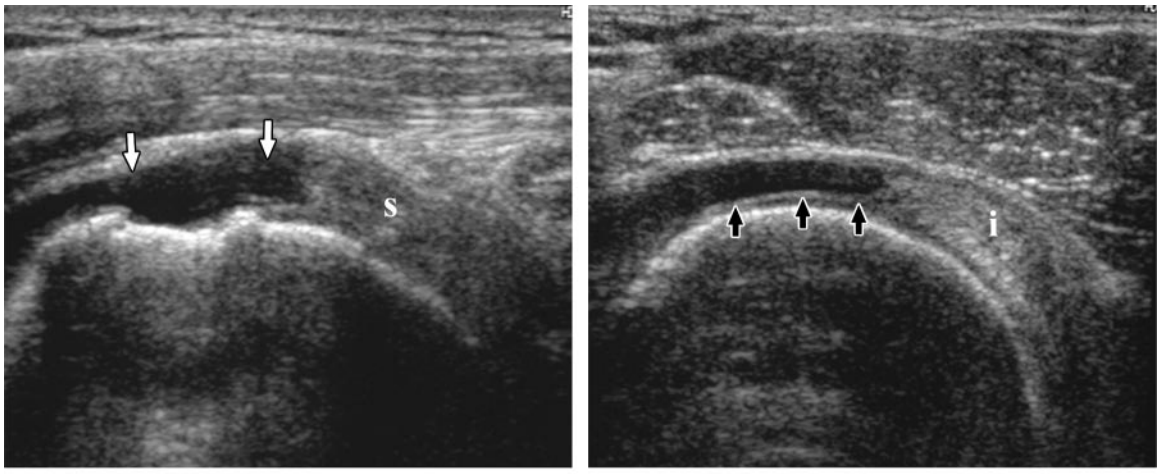

a. b.

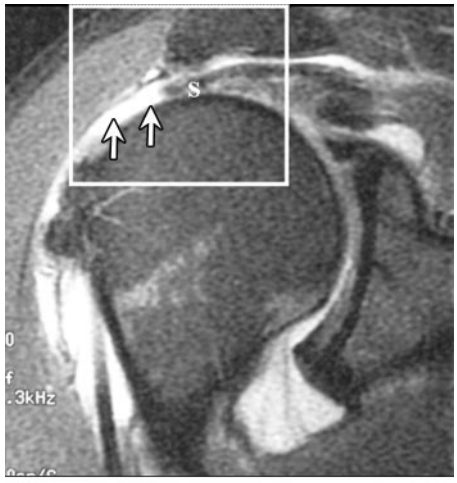

c.

Figure 18. Full-thickness tear of the supraspinatus tendon. **(a)** Longitudinal US image demonstrates a full-thickness hypoechoic defect in the normal location of the supraspinatus tendon (arrows). This defect represents fluid and extends from the bursal surface to the articular surface. Note the torn edge of the retracted supraspinatus tendon *(S)*. **(b)** Transverse US image shows an intact infraspinatus tendon *(i)* posterior to the tear. The double cortex sign can also be seen; the overlying fluid accentuates the appearance of the cartilage (arrows), which is almost as hyperechoic as the underlying cortex. **(c)** Corresponding coronal oblique fat-suppressed T2-weighted MR image shows the full-thickness defect (arrows) and the torn retracted edge of the supraspinatus tendon *(S)*. The box corresponds to the field of view in **a**.

representing the cartilage and the cortex are seen, producing the "double cortex" or "cartilage interface" sign (Fig 18b). Furthermore, compression over the focal hypoechoic defect will displace the fluid and produce loss of the normal convex contour of the peribursal fat. Loss of normal contour may be seen even without compression if there is no fluid present in the area of the torn and retracted tendon. In this situation, depression of the overlying hyperechoic peribursal fat into the tendon gap occurs, creating the "sagging peribursal fat" sign (Fig 19). Atrophy of the muscle, which manifests at US as increased echogenicity and decreased bulk of the muscle, has also been associated with tears of the tendon, with tears noted in 77% of examinations that demonstrate muscle atrophy (35). Finally, in massive tears of the supraspinatus tendon, the tendon may be retracted under the acromioclavicular joint and not visualized at US. Thus, direct signs of tear include nonvisualization of the supraspinatus tendon and hypoechoic discontinuity of the tendon, whereas indirect signs include the double cortex sign, the sagging peribursal fat sign, compressibility, and muscle atrophy.

Cortical irregularity of the greater tuberosity and shoulder joint effusion, which manifests as anechoic fluid in the axillary pouch, posterior recess, and sheath of the long head of the biceps tendon, are also considered secondary signs of rotator cuff tear (Fig 20). In fact, Jacobson et al (36) noted that the combination of these two findings at US is helpful in the diagnosis of tears, with a sensitivity of 60% and a specificity of 100%.

Partial-thickness tears manifest as focal, well-defined hypoechoic or anechoic defects in the tendon but involve only the bursal or articular surface (Fig 21). The extension of the hypoechoic defect to the bursal or articular surface should be visualized in two orthogonal imaging planes to confirm the finding. Cortical pitting and irregularity can also be seen with partial-thickness tears.

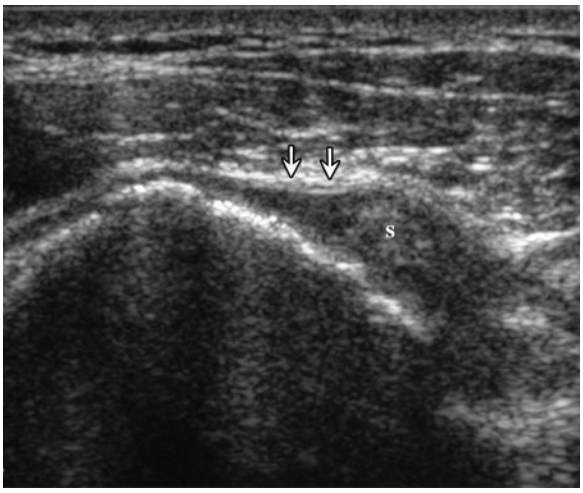

Figure 19. Sagging peribursal fat sign. Longitudinal US image shows a mildly retracted tear of the supraspinatus tendon *(S)*, with sagging of the overlying hyperechoic peribursal fat (arrows).

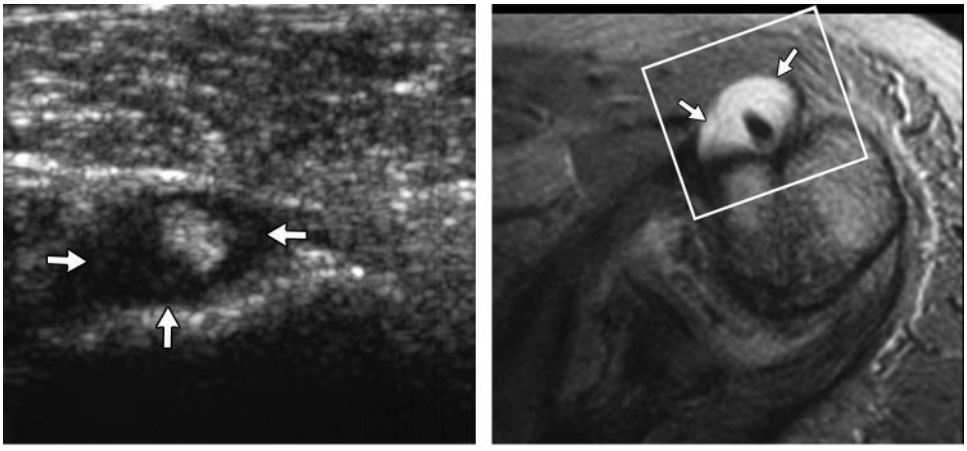

a. **b.**

Figure 20. Shoulder joint effusion tracking into the biceps tendon sheath. Transverse US image **(a)** and axial gradient-echo MR image **(b)** demonstrate an effusion in the biceps tendon sheath (arrows). The box in **b** corresponds to the field of view in **a**.

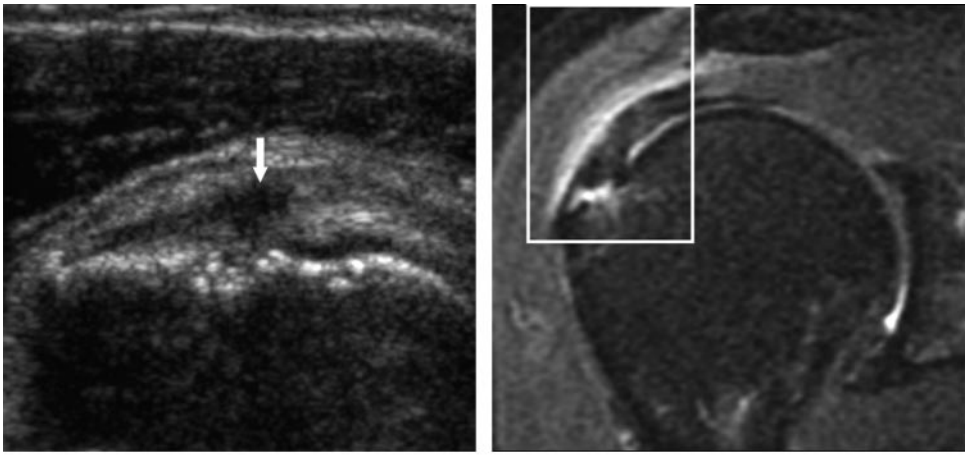

a. **b.**

Figure 21. Partial-thickness tear of the supraspinatus tendon. Longitudinal US image **(a)** and coronal oblique fat-suppressed T2-weighted MR image **(b)** show a focal, well-defined defect in the supraspinatus tendon (arrow in **a**) extending to the articular surface with cortical irregularity and a small subacromial effusion. The box in **b** corresponds to the field of view in **a**.

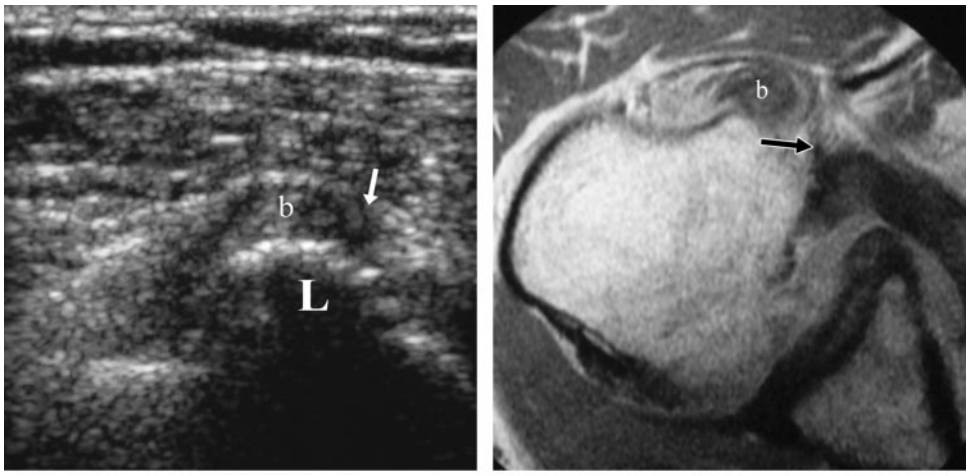

a. b.

Figure 22. Subscapularis tendon tear with subluxation of the long head of the biceps tendon. Transverse US image **(a)** and axial proton-density–weighted MR image **(b)** show a tear of the subscapularis tendon (arrow), with the biceps tendon *(b)* perched on the lesser tuberosity *(L)*.

Van Holsbeeck et al (37) reported a sensitivity and a specificity of 93% and 94%, respectively, for detection of partial-thickness tears of the rotator cuff at US.

The subscapularis tendon can also be torn, usually in combination with a supraspinatus tendon tear; isolated subscapularis tears are relatively rare (38). With rupture or articular surface tear of both the subscapularis tendon and the coracohumeral ligament, the long head of the biceps tendon can dislocate medially or become subluxated onto the lesser tuberosity (Fig 22). The biceps tendon can also become subluxated in the absence of a subscapularis tendon tear due to rupture of only the coracohumeral ligament (39,40).

Differential Diagnosis

Not all pain and weakness of the shoulder are due to rotator cuff tears, and other potential clinical mimics of rotator cuff tears, such as supraspinatus tendinosis, calcific tendinitis, subacromial subdeltoid bursitis, greater tuberosity fracture, and adhesive capsulitis, must be distinguished (39).

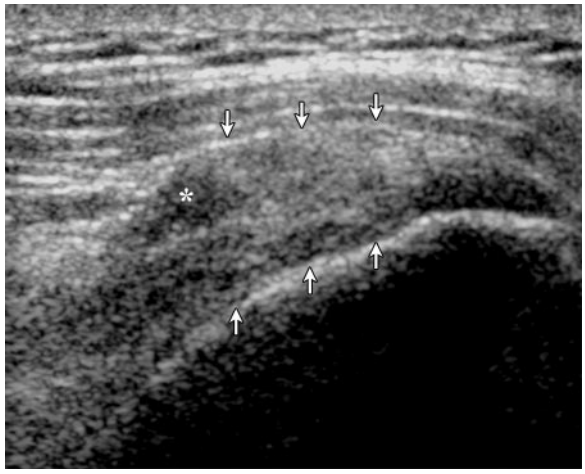

Figure 23. Tendinosis. On a longitudinal US image, the supraspinatus tendon (arrows) is thickened and heterogeneous with no discrete defects. Instead, an ill-defined hypoechoic defect with indistinct borders is seen (*).

Tendinosis represents mucoid degeneration of a tendon without inflammation. Tendinosis is radiographically occult but can be detected at US. The tendon is thickened and heterogeneous with-

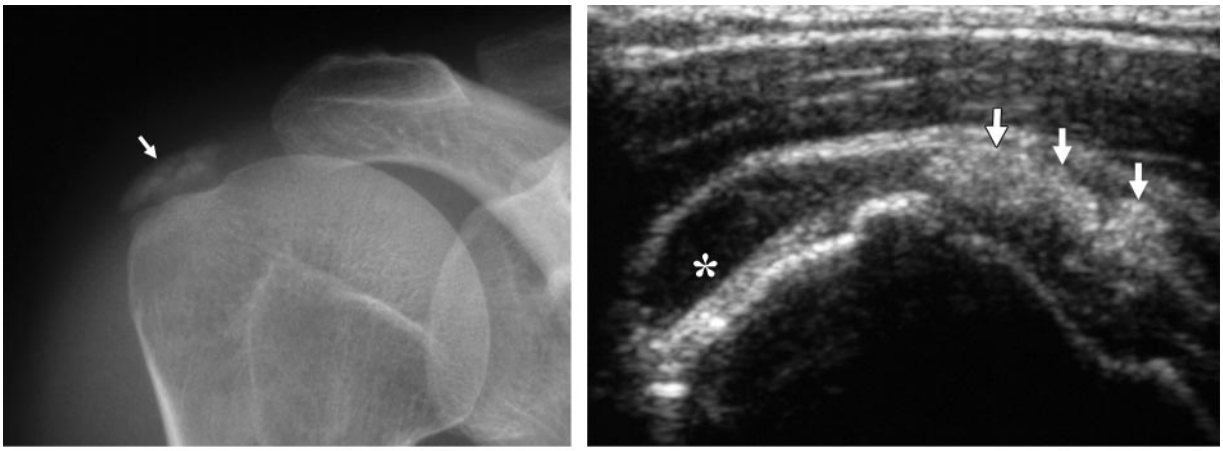

Figure 24. Calcific tendinitis. **(a)** Radiograph demonstrates deposition of calcium hydroxyapatite (arrow) just superior to the greater tuberosity at the insertion site of the supraspinatus tendon. **(b)** US image shows calcium deposition within the supraspinatus tendon as a lobular echogenic area without shadowing (arrows). Note also the effusion in the subdeltoid bursa (*).

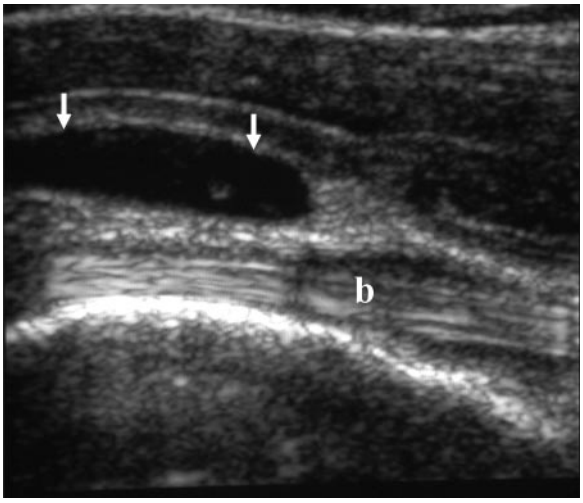

Figure 25. Subdeltoid bursitis. Longitudinal US image of the biceps tendon demonstrates a fluid collection (arrows) superficial to and not involving the biceps tendon *(b)*.

out discrete defects, and an ill-defined hypoechoic defect with indistinct borders may be present (Fig 23).

In calcific tendinitis, there is deposition of calcium hydroxyapatite within the tendon. Calcium deposition is seen in the supraspinatus tendon just superior or medial to the greater tuberosity at radiography and manifests as a discrete, linear hyperechoic focus within the tendon at US (Fig 24). Posterior acoustic shadowing may be seen at gray-scale US, and hyperemia may be seen at power Doppler US (41).

Subacromial subdeltoid bursitis is a contained collection of fluid that is superficial to the supraspinatus tendon. This inflammatory condition extends distally to the insertion of the supraspinatus tendon on longitudinal images (Fig 25) and is often seen first on transverse or sagittal images of the biceps tendon, since this is usually the first structure to be evaluated. Unlike a joint effusion, the fluid is superficial to and not within the biceps tendon sheath.

Fractures are usually radiographically evident but can also be detected at US, which depicts a fracture as a cortical step-off or discontinuity (Fig 26) (42). Cortical irregularity, however, can mimic and should not be mistaken for a fracture.

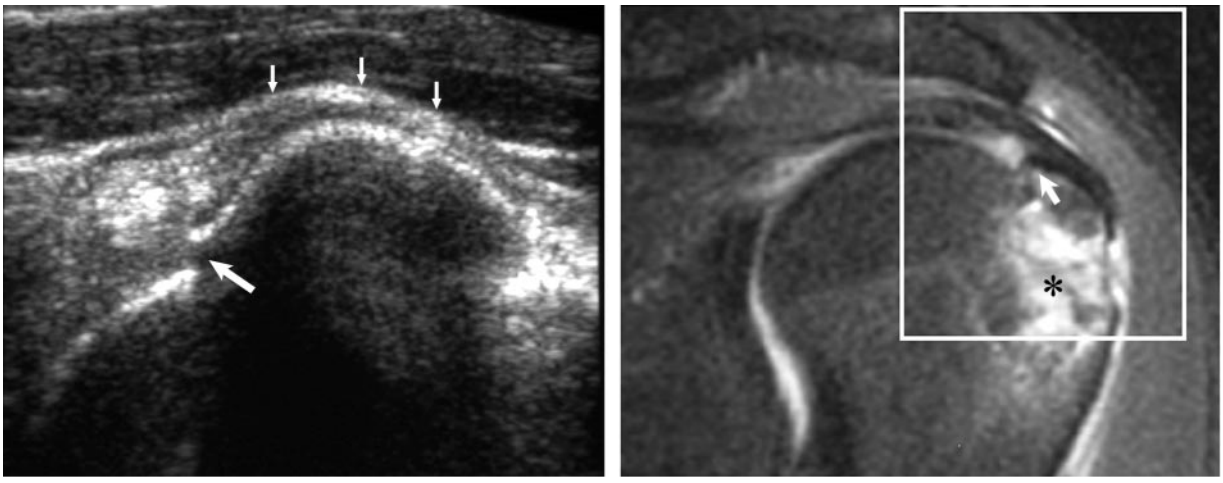

a. b.

Figure 26. Fracture. Longitudinal US image **(a)** and corresponding coronal oblique fat-suppressed T2-weighted MR image **(b)** demonstrate an intact supraspinatus tendon (small arrows in **a**) and a cortical break in the humeral head (large arrow in **a**, arrow in **b**). Adjacent high-signal-intensity bone marrow edema is evident on the MR image (*). The box in **b** corresponds to the field of view in **a**.

Adhesive capsulitis, or "frozen shoulder," is a clinical syndrome of shoulder pain, both at rest and with movement, that is caused by progressive thickening, fibrosis, and retraction of the joint capsule. Adhesive capsulitis can be distinguished clinically from rotator cuff tears on the basis of severe restriction of passive movement but can appear similar to chronic rotator cuff tears at radiography (28). At dynamic US, the diagnosis can be suggested by restriction of the sliding movement of the supraspinatus tendon underneath the acromion during abduction of the arm (43). The diagnosis can then be confirmed with arthrography, which demonstrates decreased joint volume.

Conclusions

Findings at physical examination and radiography can suggest the diagnosis of rotator cuff tear. US can help confirm the presence of rotator cuff tear and help diagnose other potential clinical mimics of this injury.

References

1. Crass JR, Craig EV, Thompson RC, Feinberg SB. Ultrasonography of the rotator cuff: surgical correlation. J Clin Ultrasound 1984;12:487–491.
2. Middleton WD, Edelstein G, Reinus WR, et al. Ultrasonography of the rotator cuff. J Ultrasound Med 1984;3:549–551.
3. Teefey SA, Rubin DA, Middleton WD, et al. Detection and quantification of rotator cuff tears: comparison of ultrasonographic, magnetic resonance imaging, and arthroscopic findings in seventy-one consecutive cases. J Bone Joint Surg Am 2004;86-A:708–716.
4. Crass JR, Craig EV, Feinberg SB. Ultrasonography of rotator cuff tears: a review of 500 diagnostic studies. J Clin Ultrasound 1988;16:313–327.
5. Zehetgruber H, Lang T, Wurnig C. Distinction between supraspinatus, infraspinatus, and subscapularis tendon tears with ultrasound in 332 surgically confirmed cases. Ultrasound Med Biol 2002;28:711–717.
6. Lyons AR, Tomlinson JE. Clinical diagnosis of tears of the rotator cuff. J Bone Joint Surg Br 1992;74:414–415.
7. Litaker D, Pioro M, El Bilbeisi H, Brems J. Returning to the bedside: using the history and physical examination to identify rotator cuff tears. J Am Geriatr Soc 2000;48:1633–1637.
8. Dinnes J, Loveman E, McIntyre L, Waugh N. The effectiveness of diagnostic tests for the assessment of shoulder pain due to soft tissue disorders: a systematic review. Health Technol Assess 2003; 7(29):iii,1–166.
9. Murrell GA, Walton JR. Diagnosis of rotator cuff tears (letter). Lancet 2001;357:769–770. [Published correction appears in Lancet 2001;357: 1452.]
10. Worland RL, Lee D, Orozco CG, et al. Correlation of age, acromial morphology, and rotator cuff tear pathology diagnosed by ultrasound in asymptomatic patients. J South Orthop Assoc 2003;12: 23–26.

11. Teefey SA, Middleton WD, Yamaguchi K. Shoulder sonography: state of the art. Radiol Clin North Am 1999;37:767–785.
12. Seibold CJ, Mallisee TA, Erickson SJ, et al. Rotator cuff: evaluation with US and MR imaging. RadioGraphics 1999;19:685–705.
13. Itoi E, Kido T, Sano A, et al. Which is more useful, the "full can test" or the "empty can test," in detecting the torn supraspinatus tendon? Am J Sports Med 1999;27:65–68.
14. Neer CS 2nd. Anterior acromioplasty for the chronic impingement in the shoulder: a preliminary report. J Bone Joint Surg Am 1972;54:41–50.
15. Zaslav KR. Internal rotation resistance strength test: a new diagnostic test to differentiate intra-articular pathology from outlet (Neer) impingement syndrome in the shoulder. J Shoulder Elbow Surg 2001;10:23–27.
16. MacDonald PB, Clark P, Sutherland K. An analysis of the diagnostic accuracy of the Hawkins and Neer subacromial impingement signs. J Shoulder Elbow Surg 2000;9:299–301.
17. Neer CS 2nd. Impingement lesions. Clin Orthop Relat Res 1983;173:70–77.
18. Hawkins RJ, Kennedy JC. Impingement syndrome in athletes. Am J Sports Med 1980;8:151–158.
19. Calis M, Akgun K, Birtane M, Karacan I, Calis H, Tuzun F. Diagnostic values of clinical diagnostic tests in subacromial impingement syndrome. Ann Rheum Dis 2000;59:44–47.
20. Gerber C, Krushell RJ. Isolated rupture of the tendon of the subscapularis muscle: clinical features in 16 cases. J Bone Joint Surg Br 1991;73:389–394.
21. Cone RO 3rd, Resnick D, Danzig L. Shoulder impingement syndrome: radiographic evaluation. Radiology 1984;150:29–33.
22. Hardy DC, Vogler JB, White RH. The shoulder impingement syndrome: prevalence of radiographic findings and correlation with response to therapy. AJR Am J Roentgenol 1986;147:557–561.
23. Bigliani LU, Ticker JB, Flatlow EL, et al. The relationship of acromial architecture to rotator cuff disease. Clin Sports Med 1991;10:823–838.
24. Peh WC, Farmer TH, Totty WG. Acromial arch shape: assessment with MR imaging. Radiology 1995;195:501–505.
25. Bloom RA. The active abduction view: a new maneuver in the diagnosis of rotator cuff tears. Skeletal Radiol 1991;20:255–258.
26. Stallenberg B, Rommens J, Legrand C, et al. Radiographic diagnosis of rotator cuff tear based on the supraspinatus muscle density. Skeletal Radiol 2001;30:31–38.
27. Kotzen LM. Roentgen diagnosis of rotator cuff tear: report of 48 surgically proven cases. Am J Roentgenol Radium Ther Nucl Med 1971;112:507–511.
28. De Smet AA, Ting YM. Diagnosis of rotator cuff tear on routine radiographs. J Can Assoc Radiol 1977;28:54–57.
29. Pearsall AW 4th, Bonsell S, Heitman RJ, et al. Radiographic findings associated with symptomatic rotator cuff tears. J Shoulder Elbow Surg 2003;12:122–127.
30. Umans HR, Pavlov H, Berkowitz M, Warren RF. Correlation of radiographic and arthroscopic findings with rotator cuff tears and degenerative joint disease. J Shoulder Elbow Surg 2001;10:428–433.
31. Bouffard JA, Lee S, Dhanju J. Ultrasonography of the shoulder. Semin Ultrasound CT MR 2000;21:164–191.
32. Crass JR, Craig EV, Bretzke C, Feinberg SB. Ultrasonography of the rotator cuff. RadioGraphics 1985;5:941–953.
33. Lin J, Fessell DP, Jacobson JA, Weadock WJ, Hayes CW. An illustrated tutorial of musculoskeletal sonography. II. Upper extremity. AJR Am J Roentgenol 2000;175:1071–1079.
34. Strobel K, Zanetti M, Nagy L, Hodler JH. Suspected rotator cuff lesions: tissue harmonic imaging versus conventional US of the shoulder. Radiology 2004;230:243–249.
35. Sofka CM, Haddad ZK, Adler RS. Detection of muscle atrophy on routine sonography of the shoulder. J Ultrasound Med 2004;23:1031–1034.
36. Jacobson JA, Lancaster S, Prasad A, et al. Full-thickness and partial-thickness supraspinatus tendon tears: value of US signs in diagnosis. Radiology 2004;230:234–242.
37. van Holsbeeck MT, Kolowich PA, Eyler WR, et al. US depiction of partial-thickness tear of the rotator cuff. Radiology 1995;197:443–446.
38. Gerber C, Hersche O, Farron A. Isolated rupture of the subscapularis tendon. J Bone Joint Surg Am 1996;78:1015–1023.
39. Martinoli C, Bianchi S, Prato N, et al. US of the shoulder: non–rotator cuff disorders. RadioGraphics 2003;23:381–401.
40. Bennett WF. Subscapularis, medial and lateral head coracohumeral ligament insertion anatomy: arthroscopic appearance and incidence of "hidden" rotator interval lesions. Arthroscopy 2001;17:173–180.
41. Chiou HJ, Chou YH, Wu JJ, et al. Evaluation of calcific tendonitis of the rotator cuff: role of color Doppler ultrasonography. J Ultrasound Med 2002;21:289–295.
42. Patten RM, Mack LA, Wang KY, Lingel J. Nondisplaced fractures of the greater tuberosity of the humerus: sonographic detection. Radiology 1992;182:201–204.
43. Ryu KN, Lee SW, Rhee YG, Lim JH. Adhesive capsulitis of the shoulder joint: usefulness of dynamic sonography. J Ultrasound Med 1993;12:445–449.

This article meets the criteria for 1.0 category 1 credit toward the AMA Physician's Recognition Award. To obtain credit, see www.rsna.org/education/rg_cme.html.